Volume 60
Number 49
21 June 2024
Pages 6213–6330

ChemComm

Chemical Communications

rsc.li/chemcomm

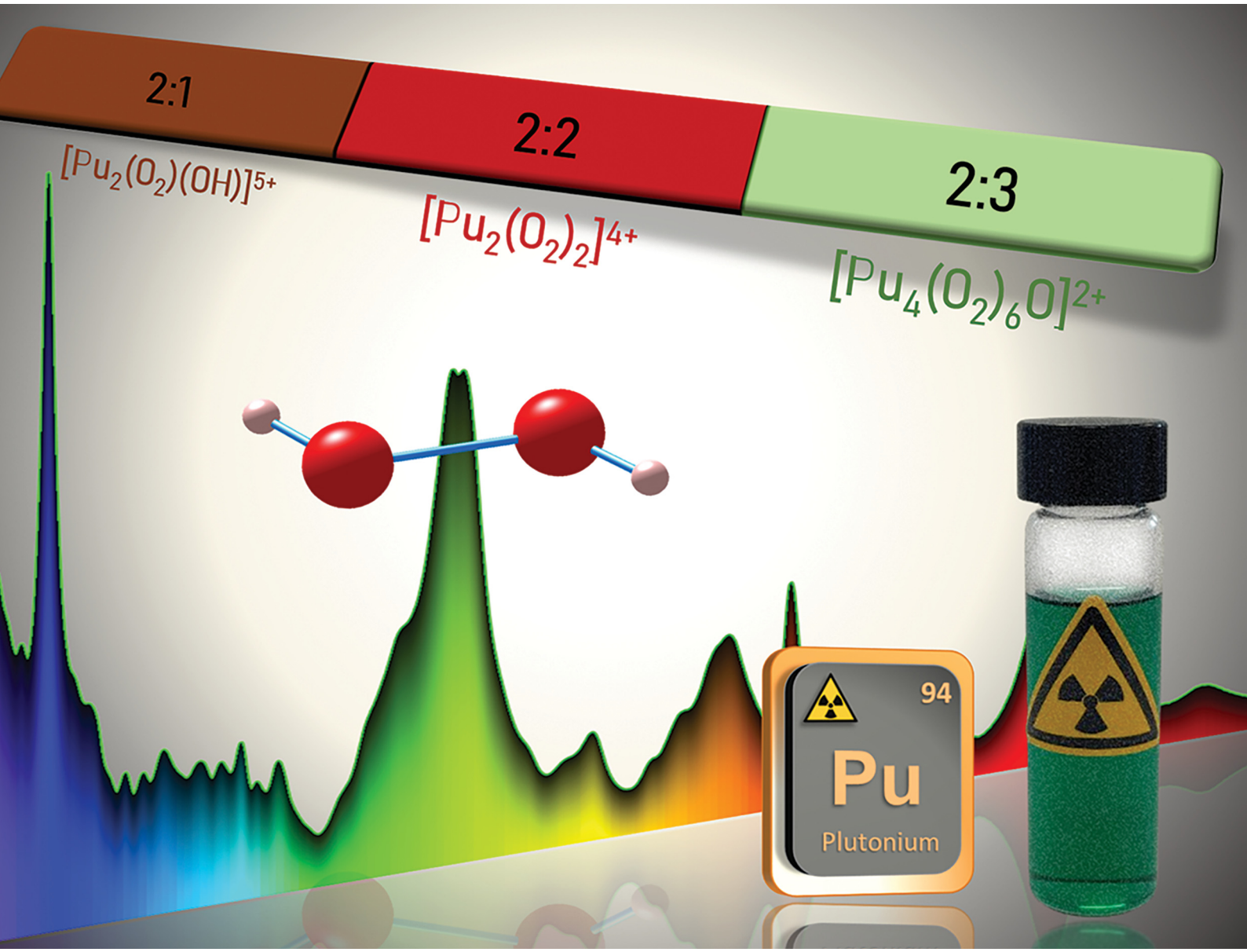

ISSN 1359-7345

ROYAL SOCIETY OF CHEMISTRY

COMMUNICATION

Matthieu Virot *et al.*

Chronicles of plutonium peroxides: spectroscopic characterization of a new peroxo compound of Pu(IV)

60 YEARS ANNIVERSARY

ChemComm

COMMUNICATION

View Article Online
View Journal | View Issue

Cite this: *Chem. Commun.*, 2024, **60**, 6260

Received 14th March 2024,
Accepted 1st May 2024

DOI: 10.1039/d4cc01186d

rsc.li/chemcomm

Chronicles of plutonium peroxides: spectroscopic characterization of a new peroxo compound of Pu(IV)†

Julien Margate,[a] Simon Bayle,[a] Thomas Dumas,[b] Elodie Dalodière,[a] Christelle Tamain,[b] Denis Menut,[c] Paul Estevenon,[b] Philippe Moisy,[b] Sergey I. Nikitenko[a] and Matthieu Virot*[a]

Although hydrogen peroxide (H_2O_2) has been highly used in nuclear chemistry for more than 75 years, the preparation and literature description of tetravalent actinide peroxides remain surprisingly scarce. A new insight is given in this topic through the synthesis and thorough structural characterization of a new peroxo compound of Pu(IV).

Peroxo-based hexavalent actinide (An) compounds have been extensively studied with the synthesis of uranyl (and neptunyl to a less extent) cage clusters and mineral compounds.[1–8] By contrast, the literature description of tetravalent An peroxides is surprisingly lacking. To date, their structural characterisation is only limited to one plutonium[9,10] and two thorium[11,12] compounds. Nevertheless, interactions between H_2O_2 and An(IV), specifically Pu, have been extensively applied since the Manhattan Project for adjusting the oxidation states, purifying the solutions, and precipitating peroxide precursors dedicated to the preparation of actinide oxides and metallic plutonium.[13]

Stoichiometric addition of H_2O_2 to acidic solutions of Pu(IV) results in the formation of the so-called "brown peroxo complex", which transitions to the "red peroxo complex" when the amount of H_2O_2 increases.[13–18] The main absorption bands for these species are located at *ca.* 494 and 658 nm for the former, and *ca.* 506 and 540 nm for the latter (Fig. 1).[13] Both complexes have been postulated to be dimers ($[Pu_2(O_2)(OH)]^{5+}$ and $[Pu_2(O_2)_2]^{4+}$ as the respectively proposed structures) that experimentally decompose in acidic solutions to yield Pu(III).[14,15,17] Further addition of H_2O_2 to Pu(IV) solutions leads to the formation of precipitates that have been used as precursors for the preparation of PuO_2 or for waste management processes.[18–20] To the best of our knowledge, structural characterisations of these compounds have never been reported in the literature. More generally, the structures and relationships occurring between Pu(IV) peroxides in solution and in the solid precipitates remain unclear to date. The only resolved structure available in the literature deals with a dimeric peroxo-carbonato compound of 10-fold coordinated Pu(IV) exhibiting two bridging μ_2:η^2-O_2 ligands and six bidentate carbonato ligands.[9,10]

In this work, the stepwise addition at room temperature of aqueous solutions of $H_2O_2$to Pu(IV) solutions previously stabilized in 2 M HNO_3 resulted in the successive formation of both the brown and red complexes ([Pu] = 5 mM, Fig. 1). The corresponding UV-Vis spectra were in good agreement with those previously reported in the literature (ESI†). Surprisingly,

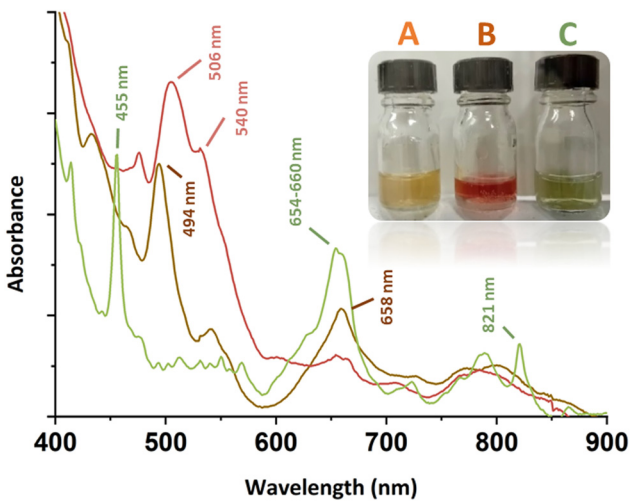

Fig. 1 Vis-NIR abs. spectra acquired in solution for the (A) brown (494, 541 and 658 nm), (B) red (506 and 540 nm) and (C) green (455, 654–660 and 821 nm) peroxo species of 5 mM Pu(IV) in nitric media. Inset: Photo of the respective solutions.

[a] *ICSM, Univ Montpellier, CEA, CNRS, ENSCM, Marcoule, France. E-mail: matthieu.virot@cea.fr*
[b] *CEA, DES, ISEC, DMRC, Univ. Montpellier, Marcoule, France*
[c] *Synchrotron SOLEIL, L'Orme des Merisiers, Saint-Aubin, France*

† Electronic supplementary information (ESI) available: Experimental details, methods, additional details and spectra. See DOI: https://doi.org/10.1039/d4cc01186d

the reverse approach, which involved diluting an aliquot of an acidic Pu(IV) solution in a large volume of an aqueous solution of concentrated H_2O_2, generated a green, limpid and very stable solution devoid of any precipitate ($[H_2O_2]/[Pu] > 10$, pH = 1–2). The corresponding electronic spectrum strongly differed not only from the spectra of the reported Pu(IV) peroxo complexes, but also from the well-known colloidal or hexanuclear cluster structures of Pu(IV) that could have been expected in such conditions as a result of hydrolysis and condensation reactions (Fig. S1, ESI†).[16,21–24] The principal features for this spectrum consist of two sharp bands attributed to f–f transitions of Pu(IV) and located at 455 and 821 nm, and a larger one standing at 654–660 nm (Fig. 1). The absence of absorption bands around 602 and 830 nm, respectively related to Pu(III) and Pu(VI), implies the absence of Pu(IV) disproportionation in the studied conditions.[22,25,26] Most probably, the band located at 455 nm is a hypsochromic shift of the Pu(IV) band generally located at 476 nm in dilute aqueous solutions of HNO_3 (Fig. S1, ESI†).

For a better understanding about the structure of this new green Pu(IV) compound, the species was precipitated at higher concentration ($[H_2O_2]/[Pu] > 10$, Pu > 10 mM, $[HNO_3] >$ 50 mM) before drying under Ar flow. Diffuse Reflectance Spectra (DRS) acquired for the powdered solid were consistent with the optical spectrum observed in the solution (Fig. 2). The good correlation between the electronic transitions observed in both the liquid and solid systems evidenced the similarity in the Pu(IV) coordination spheres for both species. This observation has led us to question the exact nature of the species in solution. Complementary filtration and ultrafiltration experiments carried out on a 1 mM Pu solution suggested the absence of a water-soluble complex, but rather the presence of a solid species with a size larger than 100 kDa (approx. 3–4 nm, Fig. S2, ESI†) that could aggregate into bigger structures (<100 nm) when increasing the concentration.

Raman spectroscopy carried out on a drop of a suspended solid in solution evidenced the characteristic signature of an

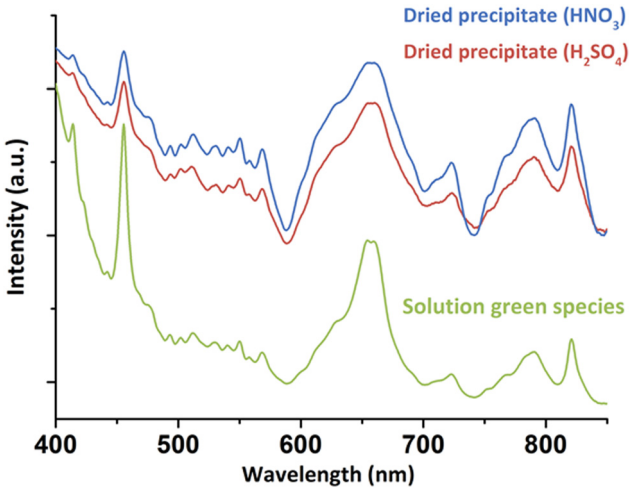

Fig. 2 DRS acquired on the solids precipitated from nitric or sulfuric Pu(IV) solutions in comparison to the green species observed in solution (nitric system).

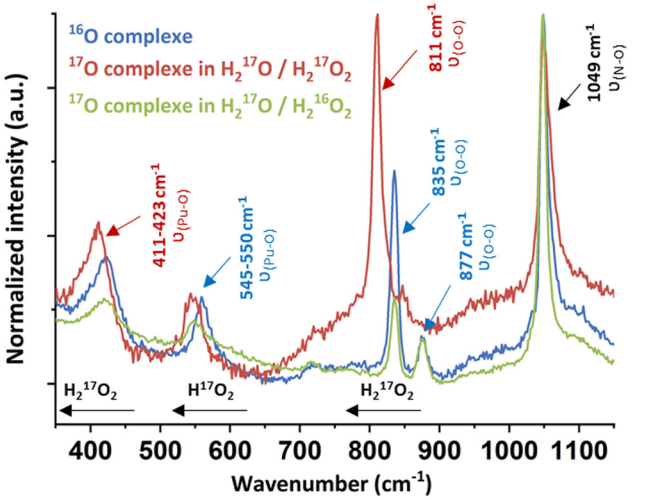

Fig. 3 Raman spectra of the green peroxo compound of Pu(IV) (nitric system) prepared in $H_2{}^{16}O/H_2{}^{16}O_2$ (blue spectrum), $H_2{}^{17}O/H_2{}^{17}O_2$ (red spectrum) and $H_2{}^{17}O/H_2{}^{16}O_2$ (green spectrum).

excess of free H_2O_2 at 877 cm^{-1} and free nitrates at 1049 cm^{-1} arising from the Pu mother solution (Fig. 3 and Fig. S3, ESI†).[11,27–31] Three additional bands located at 423, 550 and 835 cm^{-1} were investigated using mixtures of ^{17}O-marked water and H_2O_2 solutions. The use of the $H_2{}^{17}O/H_2{}^{17}O_2$ mixture involved the red shift of all of the vibration bands, except for the nitrate one (red spectrum, Fig. 3). By contrast, a $H_2{}^{17}O/H_2{}^{16}O_2$ mixture only induced the shift of a unique band initially located at 550 cm^{-1} (green spectrum, Fig. 3). This approach allowed assignment of the vibrational band located at 835 cm^{-1} (811 cm^{-1} with ^{17}O) to the ν(O–O) symmetric stretching vibration mode of the peroxide ligand that shifts in comparison to pure H_2O_2 because of Pu atom(s) coordination (ESI†).

The Raman band located at 423 cm^{-1} (411 cm^{-1} with ^{17}O) was attributed to the ν(Pu–O) vibrational mode of the peroxide group. A similar signature has been observed for other An or Ce peroxo species exhibiting bridging μ_2-η^2:η^2 or μ_3-η^2:η^2:η^2 coordination modes.[10,11,27] The band located at 550 cm^{-1} could not be clearly identified using this approach, but it is not related to the peroxide group(s) due to the significant shift of the band when using a $H_2{}^{17}O/H_2{}^{16}O_2$ mixture. Most probably, this band relates to oxo or hydroxo group(s) coordinating Pu atoms. Synthesizing the green Pu compound in a D_2O/H_2O mixture did not help in the functional group(s) identification. Nevertheless, we note that the T_{2g} band for An dioxides is located around this area (465 cm^{-1} for ThO_2, 445 cm^{-1} for UO_2 or 478 cm^{-1} for PuO_2).[32] The T_{2g} band represents the antisymmetric stretching of the Pu–μ_4O bonds in the cubic structure and is highly affected by the bond strength and local environment, suggesting a possible assignment of this band to oxo group(s).[33]

Interestingly, the synthesis of the green peroxo compound at pH = 2.3 with a Pu(IV) solution previously stabilized in sulphuric medium did not lead to a stable solution, but quickly precipitated. DRS and Raman spectroscopies showed similar band

positions with the nitrate system for both solid and concentrated liquid states (Fig. 2 and Fig. S3, ESI†). One exception is the vibrational band located at 994 cm^{-1} in Raman spectroscopy and attributed to $\nu_1(SO_4)$ of free sulphate ions.[34] These observations suggested similar structures for both nitric and sulfuric systems, but also a possible absence of participation of the counter-ion in the coordination sphere of Pu in the solution or in the precipitate. Fourier Transform Infra-Red (FT-IR) spectroscopy on the solids obtained in both nitric and sulfuric media showed the characteristic signatures of nitrates,[29,35] sulphates[34,36] and interstitial and/or coordinated water molecules (Fig. S4, ESI†).[37,38] The presence of the peroxo group(s) was confirmed with the weak bands located at 832–833 cm^{-1} for both media.[11,39] The observation of peroxo bands for both vibrational spectroscopies (assigned to the ν(O–O) symmetric stretching vibration mode) agrees with the bridging coordination modes already observed for other Zr(IV), Ce(IV), U(VI), Th(IV) and Pu(IV) peroxo compounds.[7,9–11,40,41]

Solids obtained in the presence of sulphate and nitrate ions provided similar X-ray diffraction patterns, indicating similar crystalline structures (Fig. 4(a)), finally tending to stipulate (considering Raman and UV-vis spectroscopies) that the counter ions do not enter the Pu coordination spheres. Thermogravimetric analyses carried out on both solids obtained from the nitric and sulphuric systems (Fig. S5, ESI†) evidenced three domains attributed to the release of H_2O molecules (<125 °C), followed by the decomposition of O_2^{2-} ligands (125–225 °C) and the decomposition of nitrates (>225 °C) or sulfates (>550 °C).[11,13,38,42] Mass loss calculations confirmed a double amount of NO_3^- in comparison to SO_4^{2-}, assuming that the Pu core of the green peroxo compound exhibits a positive charge of +2 (ESI†).

X-ray absorption near edge structure (XANES) obtained at the Pu L_3-edge in solution for the green peroxo compound evidenced the predominance of the +IV oxidation state (Fig. S6, ESI†). The experimental k^3-weighted extended X-ray absorption fine structure (EXAFS) spectrum obtained in the 3–16 $Å^{-1}$ interval is provided in Fig. S7a (ESI†). The corresponding Fourier transform (FT) magnitude in black in Fig. 4(b) (uncorrected for phase shift) showed two large peaks standing at $R - \phi$ = 1.9 and 3.5 Å attributed to the Pu–O and Pu–Pu coordination spheres. The latter was adjusted at 3.65 Å (CN = 3.6(7)), indicating the formation of a polynuclear structure. Such a Pu–Pu distance does not correspond to any structure available in the literature (Fig. 4(c)), thus excluding peroxide dimers[9] (3.53 Å), oxo-hydroxo hexamers[24] (3.77 Å) or PuO_2-like structures[43] (3.81 Å). The absence of a secondary Pu–Pu distance combined with the data acquired using different techniques (charge +2, several Pu–O bonds, CN_{Pu-Pu}, bridging mode peroxides, no counter-ion in the structure) led us to propose a hypothetical structure inspired by Th, U and Pa tetrahedral arrangements.[44,45] Consequently, three Pu–O subshells were adjusted using a short distance (*ca.* 2.2 Å) corresponding to a μ_4-O group, an intermediate distance for the peroxide groups (*ca.* 2.3 Å agreeing with Runde *et al.*[9]) and a longer one (*ca.* 2.45 Å) for H_2O molecules. The successful fit for this spectrum was achieved using free contributions (blue fit, Fig. 4(b)) with structural parameters at 2.14 Å (CN = 1.3(5)), 2.32 Å (CN = 6.5(6)) and 2.45 Å (CN = 3.5(7)) for the Pu–O sphere (ESI†). Hence, the resulting hypothetical unit pattern agrees with the formula $[Pu_4(O_2)_6(O)(H_2O)_{12}]_n^{2+}$ provided in Fig. S8 (ESI†).

The latter is a unitary tetrameric pattern involving four Pu atoms located at the corner of a tetrahedron. The unit incorporates a μ_4-O atom and is coordinated with six μ_2-O_2 ligands standing on each edge. The μ_4-oxo position is reminiscent of the one observed in bulk PuO_2. H_2O molecules then stand around the Pu atoms to complete the coordination sphere, in agreement with previous Th and Pu peroxo structures (CN = 10).[9,46] By using the atom coordinates (CrystalMaker Software Ltd), scattering paths were generated and structural parameters were calculated (ESI†). The as-obtained parameters and related FT (Fig. 4(b), orange fit and Fig. S7b, ESI†) were in very good agreement with the experimental EXAFS spectrum giving weight to the hypothetical structure. The most intriguing question deals with the Pu–O distance observed for the μ_4-oxo group (2.13 Å), which is much smaller than that observed in bulk PuO_2 (2.33 Å).[43] The tetrahedral units reported for both

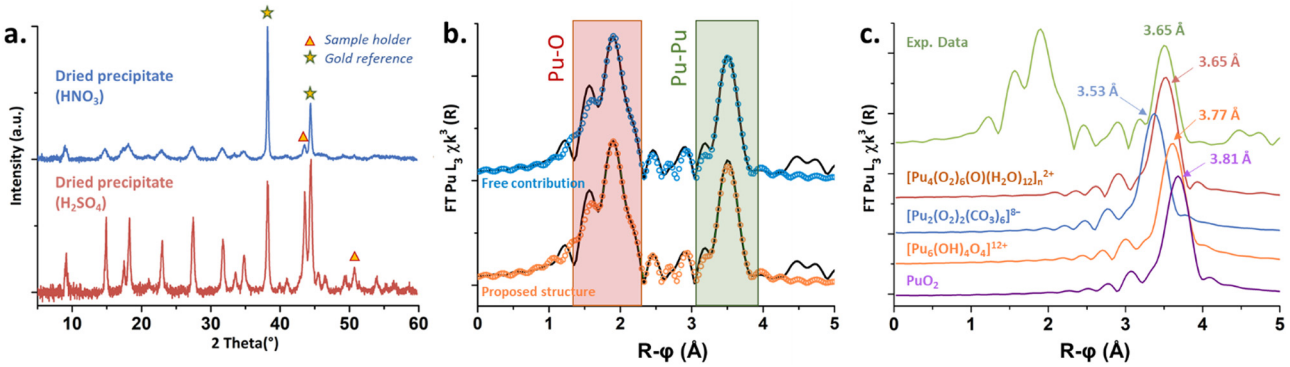

Fig. 4 (a) XRD diffractograms for the green peroxo precipitated from Pu(IV) stabilized in HNO_3 or H_2SO_4 media. (b) FT of the experimental k^3-weighted EXAFS spectrum (black) measured on the green compound in solution (5 mM). Blue and orange circles stand for the fits. (c) Plot of the normalized Pu–Pu contributions observed on the FT EXAFS spectra for different Pu-based polynuclear structures in comparison to the experimental data (green) and the hypothetical structure (red).

Th(IV) and U(IV) compounds (ESI†) showed strongly split distances for the An–μ_4O group incorporating at the same time shorter and longer distances when compared to the respective bulk oxides. In addition, such structures allow the possible observation of much shorter An–An distances in comparison to the one observed in the respective bulk oxides (3.74 Å and 3.52 Å for Th and U, against 3.97 Å and 3.87 Å for the respective oxides). These observations could agree and explain the nature of the shifted Raman band located at 550 cm^{-1} on Fig. 3, thus strengthening our proposition. Furthermore, it is worth noting that the mass losses calculations performed with the hypothetical and (+2) positively charged structure (Table S4, ESI†) well agreed with the experimental thermograms for both nitric and sulfuric systems with 2% or 0.4% error, respectively (can be improved with 10 H_2O molecules instead of 12).

This newly-discovered green Pu(IV) compound fills the poor library available about tetravalent An peroxides. The distinct spectroscopic and structural characteristics of the associated polynuclear structure of Pu(IV) shed a new light on our overall knowledge on An peroxides and their potential applications in nuclear chemistry and materials preparation. Further investigations are imperative to unravel the precise structures and properties of the Pu(IV) peroxide species, including the brown and red ones. While these results offer insights into the first coordination sphere of Pu for the green peroxo compound, the long-range structure in the solution (cluster, polymer, colloid...) or in the precipitated solid remains undefined and deserves further investigation.

Conflicts of interest

There are no conflicts to declare.

References

1 P. C. Burns, K. A. Kubatko, G. Sigmon, B. J. Fryer, J. E. Gagnon, M. R. Antonio and L. Soderholm, *Angew. Chem., Int. Ed.*, 2005, **44**, 2135–2139.
2 B. Vlaisavljevich, L. Gagliardi and P. C. Burns, *J. Am. Chem. Soc.*, 2010, **132**, 14503–14508.
3 K. A. H. Kubatko, K. B. Helean, A. Navrotsky and P. C. Burns, *Science*, 2003, **302**, 1191–1193.
4 F. Clarens, J. De Pablo, I. Diez-Perez, I. Casas, J. Gimenez and M. Rovira, *Environ. Sci. Technol.*, 2004, **38**, 6656–6661.
5 C. R. Armstrong, M. Nyman, T. Shvareva, G. E. Sigmon, P. C. Burns and A. Navrotsky, *Proc. Natl. Acad. Sci. U. S. A.*, 2012, **109**, 1874–1877.
6 M. Nyman, M. A. Rodriguez and C. F. Campana, *Inorg. Chem.*, 2010, **49**, 7748–7755.
7 J. Qiu and P. C. Burns, *Chem. Rev.*, 2013, **113**, 1097–1120.
8 S. Hickam, D. Ray, J. E. S. Szymanowski, R. Y. Li, M. Dembowski, P. Smith, L. Gagliardi and P. C. Burns, *Inorg. Chem.*, 2019, **58**, 12264–12271.
9 W. Runde, L. F. Brodnax, G. S. Goff, S. M. Peper, F. L. Taw and B. L. Scott, *Chem. Commun.*, 2007, 1728–1729.
10 L. E. Sweet, J. F. Corbey, F. Gendron, J. Autschbach, B. K. McNamara, K. L. Ziegelgruber, L. M. Arrigo, S. M. Peper and J. M. Schwantes, *Inorg. Chem.*, 2017, **56**, 791–801.
11 L. Bonato, M. Virot, T. Dumas, A. Mesbah, P. Lecante, D. Prieur, X. Le Goff, C. Hennig, N. Dacheux, P. Moisy and S. I. Nikitenko, *Chem. – Eur. J.*, 2019, **25**, 9580–9585.
12 S. S. Galley, C. E. Van Alstine, L. Maron and T. E. Albrecht-Schmitt, *Inorg. Chem.*, 2017, **56**, 12692–12694.
13 J. A. Leary, A. N. Morgan and W. J. Maraman, *Ind. Eng. Chem.*, 1959, **51**, 27–31.
14 A. S. Mazumdar, P. R. Nataraja and S. Vaidyana, *J. Inorg. Nucl. Chem.*, 1970, **32**, 3363–3367.
15 C. Maillard and J. M. Adnet, *Radiochim. Acta*, 2001, **89**, 485–490.
16 R. E. Connick and W. H. Mcvey, *J. Am. Chem. Soc.*, 1949, **71**, 1534–1542.
17 A. Ekstrom and A. McLaren, *J. Inorg. Nucl. Chem.*, 1972, **34**, 1009–1016.
18 G. Daniel, Literature review of PuO_2 calcination time and temperature data for specific surface area, United States, 2012.
19 S. F. Marsh and T. D. Gallegos, Chemical treatment of plutonium with hydrogen peroxide before nitrate anion exchange processing. [Reduction to (IV)], Report LA-10907, 1987.
20 P. G. Hagan and F. J. Miner, *Plutonium peroxide precipitation: review and current research*, American Chemical Society, United States, 1980.
21 T. Dumas, M. Virot, D. Menut, C. Tamain, C. Micheau, S. Dourdain and O. Diat, *J. Synchrotron Radiat.*, 2022, **29**, 30–36.
22 M. Cot-Auriol, M. Virot, T. Dumas, O. Diat, D. Menut, P. Moisy and S. I. Nikitenko, *Chem. Commun.*, 2022, **58**, 13147–13150.
23 G. Chupin, C. Tamain, T. Dumas, P. L. Solari, P. Moisy and D. Guillaumont, *Inorg. Chem.*, 2022, **61**, 4806–4817.
24 C. Tamain, T. Dumas, D. Guillaumont, C. Hennig and P. Guilbaud, *Eur. J. Inorg. Chem.*, 2016, 3536–3540.
25 D. Clark, S. Hecker, G. Jarvinen and M. Neu, in *The Chemistry of the Actinide and Transactinide Elements*, ed. L. Morss, N. Edelstein and J. Fuger, Springer, Netherlands, 2011, ch. 7, pp. 813–1264, DOI: 10.1007/978-94-007-0211-0_7.
26 E. Dalodière, M. Virot, T. Dumas, D. Guillaumont, M. C. Illy, C. Berthon, L. Guerin, A. Rossberg, L. Venault, P. Moisy and S. I. Nikitenko, *Inorg. Chem. Front.*, 2018, **5**, 100–111.
27 B. T. McGrail, G. E. Sigmon, L. J. Jouffret, C. R. Andrews and P. C. Burns, *Inorg. Chem.*, 2014, **53**, 1562–1569.
28 A. A. Mikhaylov, A. G. Medvedev, A. V. Churakov, D. A. Grishanov, P. V. Prikhodchenko and O. Lev, *Chem. – Eur. J.*, 2016, **22**, 2980–2986.
29 U. Casellato, P. A. Vigato and M. Vidali, *Coord. Chem. Rev.*, 1981, **36**, 183–265.
30 S. Gajaraj, C. Fan, M. Lin and Z. Hu, *Environ. Monit. Assess.*, 2013, **185**, 5673–5681.
31 Y. Suffren, F.-G. Rollet and C. Reber, *Comments Inorg. Chem.*, 2011, **32**, 246–276.
32 G. M. Begun, R. G. Haire, W. R. Wilmarth and J. R. Peterson, *J. Less-Common Met.*, 1990, **162**, 129–133.
33 E. Epifano, M. Naji, D. Manara, A. C. Scheinost, C. Hennig, J. Lechelle, R. J. M. Konings, C. Guéneau, D. Prieur, T. Vitova, K. Dardenne, J. Rothe and P. M. Martin, *Commun. Chem.*, 2019, **2**, 59.
34 K. Ben Mabrouk, T. H. Kauffmann, H. Aroui and M. D. Fontana, *J. Raman Spectrosc.*, 2013, **44**, 1603–1608.
35 M. Y. Mihaylov, V. R. Zdravkova, E. Z. Ivanova, H. A. Aleksandrov, P. S. Petkov, G. N. Vayssilov and K. I. Hadjiivanov, *J. Catal.*, 2021, **394**, 245–258.
36 D. E. Chasan and G. Norwitz, Infrared determination of inorganic sulfates and carbonates by the pellet technique, Report Test Report T69-10-1, 1969.
37 C. R. Bhattacharjee, M. K. Chaudhuri, S. K. Chettri and J. J. Laiwan, *J. Fluorine Chem.*, 1994, **66**, 229–231.
38 M. Falk and T. A. Ford, *Can. J. Chem.*, 1966, **44**, 1699–1707.
39 J. A. Leary, U. S. A. E. Commission and L. A. S. Laboratory, Studies on the Preparation, Properties, and Composition of Plutonium Peroxide, Los Alamos Scientific Laboratory of the University of California, 1954.
40 G. V. Jere and G. D. Gupta, *J. Inorg. Nucl. Chem.*, 1970, **32**, 537–542.
41 G. V. Jere and M. T. Santhamma, *Inorg. Chim. Acta*, 1977, **24**, 57–61.
42 N. Hibert, B. Arab-Chapelet, M. Rivenet, L. Venault, C. Tamain and O. Tougait, *Dalton Trans.*, 2022, **51**, 12928–12942.
43 M. Virot, T. Dumas, M. Cot-Auriol, P. Moisy and S. I. Nikitenko, *Nanoscale Adv.*, 2022, **4**, 4938–4971.
44 K. E. Knope and L. Soderholm, *Chem. Rev.*, 2013, **113**, 944–994.
45 R. E. Wilson, S. De Sio and V. Vallet, *Nat. Commun.*, 2018, **9**, 622.
46 L. Bonato, M. Virot, X. Le Goff, P. Moisy and S. I. Nikitenko, *Ultrason. Sonochem.*, 2020, **69**, 105235.